iScience

CellPress
OPEN ACCESS

Article

Bridging large-scale cortical networks: Integrative and function-specific hubs in the thalamus

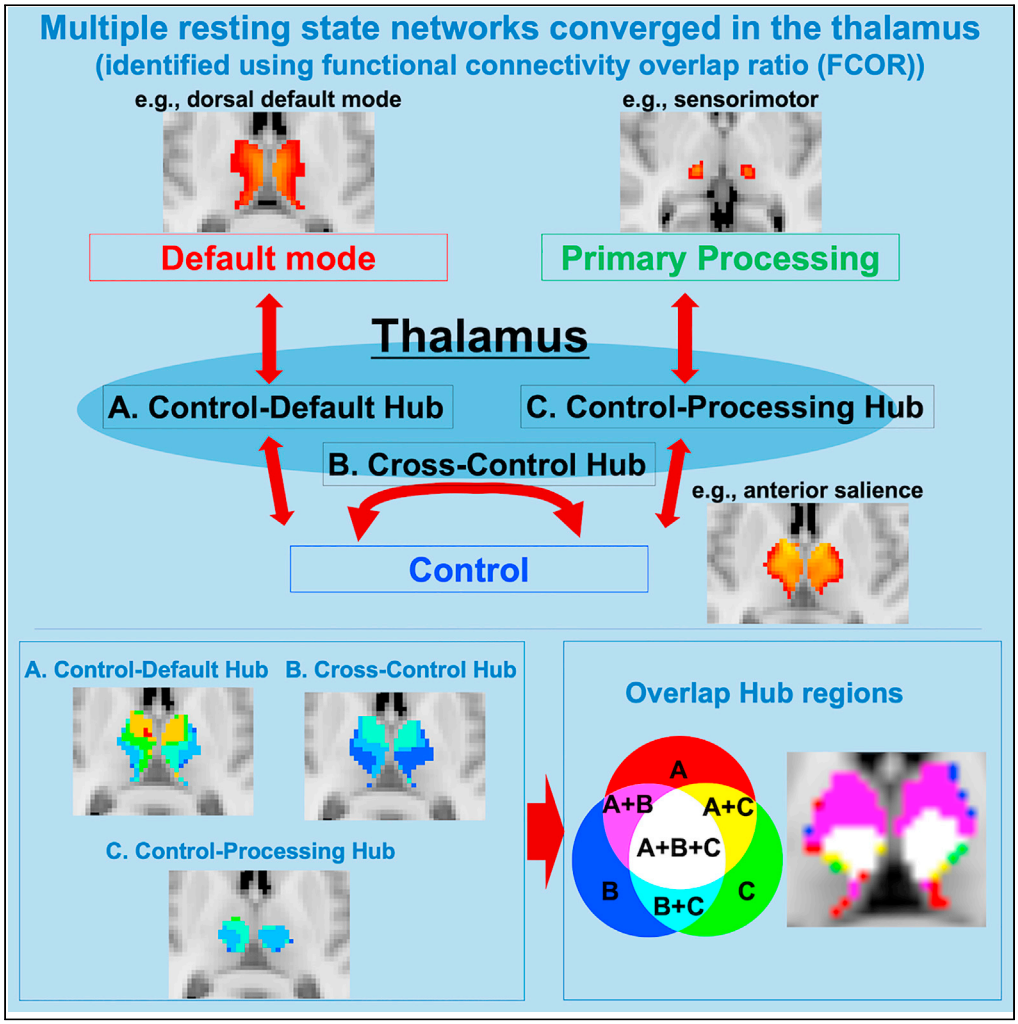

Kazuya Kawabata, Epifanio Bagarinao, Hirohisa Watanabe, ..., Shinji Naganawa, Norio Ozaki, Gen Sobue

nabe@med.nagoya-u.ac.jp (H.W.)
sobueg@med.nagoya-u.ac.jp (G.S.)

Highlights

Multiple large-scale cortical networks converged in the thalamus

Neurocognitive associated hub existed in the anterior and medial region

Control-processing hub localized in the intermediate thalamus

Sensorimotor network was located around the lateral pulvinar nucleus

Kawabata et al., iScience 24, 103106
October 22, 2021
https://doi.org/10.1016/j.isci.2021.103106

iScience

CellPress
OPEN ACCESS

Article

Bridging large-scale cortical networks: Integrative and function-specific hubs in the thalamus

Kazuya Kawabata,[1,2] Epifanio Bagarinao,[2,3] Hirohisa Watanabe,[2,4,10,*] Satoshi Maesawa,[2,5] Daisuke Mori,[2] Kazuhiro Hara,[1] Reiko Ohdake,[2,4] Michihito Masuda,[1] Aya Ogura,[1] Toshiyasu Kato,[1] Shuji Koyama,[2,3] Masahisa Katsuno,[1] Toshihiko Wakabayashi,[5] Masafumi Kuzuya,[6] Minoru Hoshiyama,[2,3] Haruo Isoda,[2,3] Shinji Naganawa,[7] Norio Ozaki,[2,8] and Gen Sobue[2,9,*]

SUMMARY

The thalamus is critical for the brain's integrative hub functions; however, the localization and characterization of the different thalamic hubs remain unclear. Using a voxel-level network measure called functional connectivity overlap ratio (FCOR), we examined the thalamus' association with large-scale resting-state networks (RSNs) to elucidate its connector hub roles. Connections to the core-neurocognitive networks were localized in the anterior and medial parts, such as the anteroventral and mediodorsal nuclei areas. Regions functionally connected to the sensorimotor network were distinctively located around the lateral pulvinar nucleus but to a limited extent. Prominent connector hubs include the anteroventral, ventral lateral, and mediodorsal nuclei with functional connections to multiple RSNs. These findings suggest that the thalamus, with extensive connections to most of the RSNs, is well placed as a critical integrative functional hub and could play an important role for functional integration facilitating brain functions associated with primary processing and higher cognition.

INTRODUCTION

The thalamus is a nuclear complex consisting of dozens of nuclei located in the diencephalon. The thalamus has been traditionally considered as a relay station in the flow of various sensory signals. More recent evidence, however, has shown that the thalamus has roles in connecting sensory and cognitive processing (Sherman, 2016; Wolff et al., 2020). Based on animal studies, Sherman categorized thalamic relays into two types based on their inputs: first-order relays, which receive subcortical driver input, and higher-order relays, which receive input from layer 5 of the cortex and participate in cortico-thalamocortical circuits (Sherman, 2016). The presence of these higher-order relays involved in transthalamic corticocortical communications suggests that the thalamus continues to participate in the processing of information within cortical hierarchies. Citing the role of the thalamic reticular nucleus and modulator inputs to the thalamus, Wolff and colleagues further proposed that the thalamus as a whole, including both first-order and higher-order nuclei, may be critical for integrating environmental signals in cognitive processes and thus serving as a bridge linking sensory perception and cognition (Wolff et al., 2020). Although cortical circuitries associated with cognition have been well studied, the role of the thalamus in cognitive processes is just beginning to be elucidated (Halassa and Kastner, 2017).

Using neuroimaging, several studies have examined both the anatomical and functional organization of the thalamus in humans. Recent investigations using resting-state functional magnetic resonance imaging (fMRI) have also indicated that the thalamus and basal ganglia connect to several cortical functional networks and contribute to multimodal cognitive functions (Bell and Shine, 2016; Greene et al., 2020). Graph-theoretic network analysis revealed that several thalamic subdivisions have network properties capable of integrating information across multiple cortical functional networks (Hwang et al., 2017). With widespread structural and functional connectivity to the cerebral cortex, the thalamus is well positioned to mediate the interactions between distributed, large-scale cortical functional networks, which may be associated with higher brain functions (Shine, 2020).

[1]Department of Neurology, Nagoya University Graduate School of Medicine, Nagoya, Aichi, Japan

[2]Brain and Mind Research Center, Nagoya University, Tsurumai-cho, Showa-ku, Nagoya, Aichi, Japan

[3]Department of Integrated Health Sciences, Nagoya University Graduate School of Medicine, Nagoya, Aichi, Japan

[4]Department of Neurology, Fujita Health University School of Medicine, Dengakugakubo, Kutsukake-cho, Toyoake, Aichi, Japan

[5]Department of Neurosurgery, Nagoya University Graduate School of Medicine, Nagoya, Aichi, Japan

[6]Department of Community Healthcare and Geriatrics, Nagoya University Graduate School of Medicine and Institutes of Innovation for Future Society, Nagoya University, Nagoya, Aichi, Japan

[7]Department of Radiology, Nagoya University Graduate School of Medicine, Nagoya, Aichi, Japan

[8]Department of Psychiatry, Nagoya University Graduate School of Medicine, Nagoya, Aichi, Japan

[9]Aichi Medical University, Nagakute, Aichi, Japan

[10]Lead contact

*Correspondence: nabe@med.nagoya-u.ac.jp (H.W.), sobueg@med.nagoya-u.ac.jp (G.S.)

https://doi.org/10.1016/j.isci.2021.103106

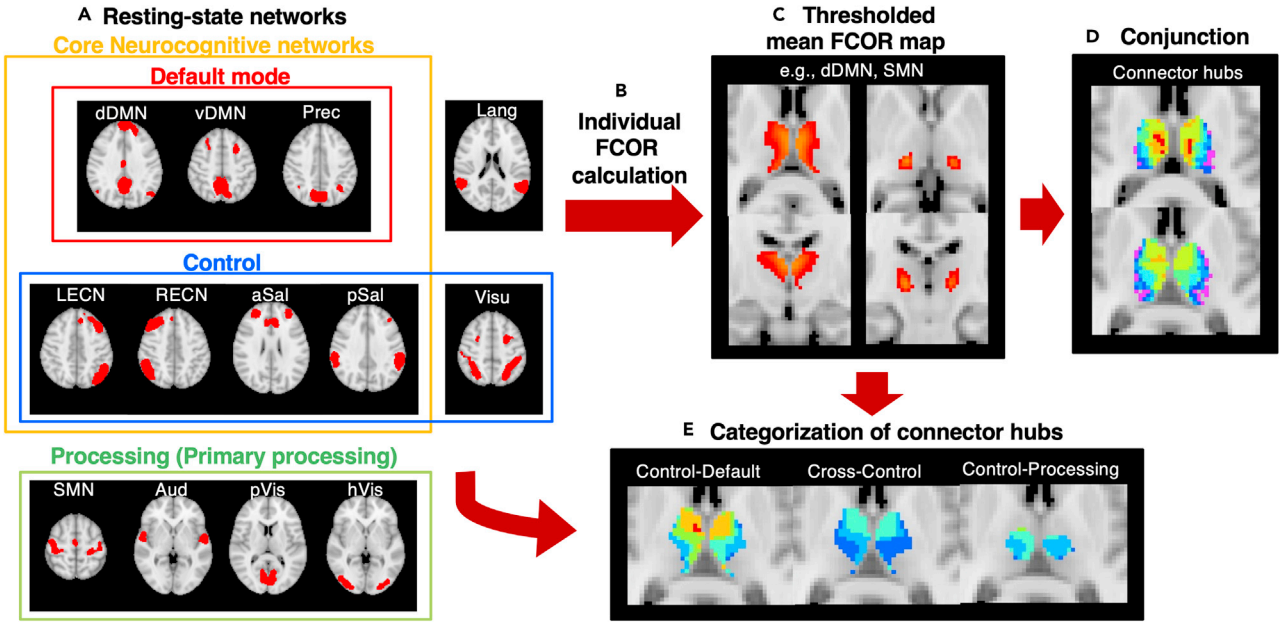

Figure 1. Outline of the approach to identify and further categorize thalamic connector hubs

(A) The different large-scale resting-state networks (RSNs) in the Shirer atlas. These RSNs were further grouped into 3 general classifications, namely default (red), control (blue), and processing (green) networks, which was used to additionally categorize connector hubs. The termed core neurocognitive networks (Menon, 2011; Seeley et al., 2007) was also used for RSNs primarily involved in cognitive processing (default, salience, and executive control networks). dDMN, dorsal default mode network; vDMN, ventral default mode network; Prec, precuneus network; LECN, left executive control network; RECN, right executive control network; aSal, anterior salience network; pSal, posterior salience network; Lang, language network; Visu, visuospatial (dorsal attention) network; pVis, primary visual network; hVis, higher visual network; Aud, auditory network; SMN, sensorimotor network.

(B) Using these RSNs as reference, the individual FCOR maps associated with each RSN were then constructed. The approach is detailed in the STAR Methods section and in our previous paper (Bagarinao et al., 2020).

(C) Individually constructed maps for each RSN were averaged across all participants and thresholded at 0.1 (10%).

(D) A conjunction analysis applied to the thresholded FCOR maps was used to identify regions that are connected to multiple RSNs. These regions represent connector hubs in the thalamus.

(E) Connector hubs were further categorized into control-default, cross-control, and control-processing (Bagarinao et al., 2020; Gordon et al., 2018) by identifying overlap regions between FCOR maps of control and default mode networks, two or more control networks, and control and processing networks, respectively.

To elucidate the thalamus' integrative functional role, it is necessary to fully understand the thalamus' association with large-scale functional brain networks, which can be considered the brain's functional modules. Considering that thalamic dysfunction is at the core of numerous psychiatric pathologies with varying clinical manifestations such as major depressive disorder, obsessive compulsive disorder, bipolar disorder, and schizophrenia, among others (Parnaudeau et al., 2018), understanding this functional association would be extremely valuable to characterize these dysfunctions. The goal of this paper is to examine this association comprehensively, identify multi-network integrative hub locations in the thalamus, and clarify the connectivity properties of the identified hub regions. To achieve this, we used a voxel-level functional connectivity (FC) measure called functional connectivity overlap ratio (FCOR) that can be used to quantify the spatial extent of a voxel's connection to several well-known large-scale cortical functional networks (Bagarinao et al., 2020). In our previous report, we successfully obtained voxel-level FCOR measurement to the whole-brain FC to identify cortical connector hubs. Here, we focused on the thalamus' connectivity to the cortex and investigated the extent of each thalamic voxel's connection to the various functional networks, which can provide a more in-depth understanding of the voxel's functional role. The distribution of the thalamic connector hubs was then identified using voxels with extensive connections with not just one but multiple networks (Figure 1). Using the general classification of cortical networks into default mode (e.g. the dorsal and ventral default mode networks), control (e.g., the salience and executive control networks), and processing networks (e.g., the sensorimotor and auditory networks), we further categorized the thalamic connector hub voxels into control-default, cross-control, and control-processing hubs (Bagarinao et al., 2020; Gordon et al., 2018). We also parcellated the thalamus into functional subcomponents using FCOR values to identify regions primarily associated with primary processing from those involved in higher cognitive processes.

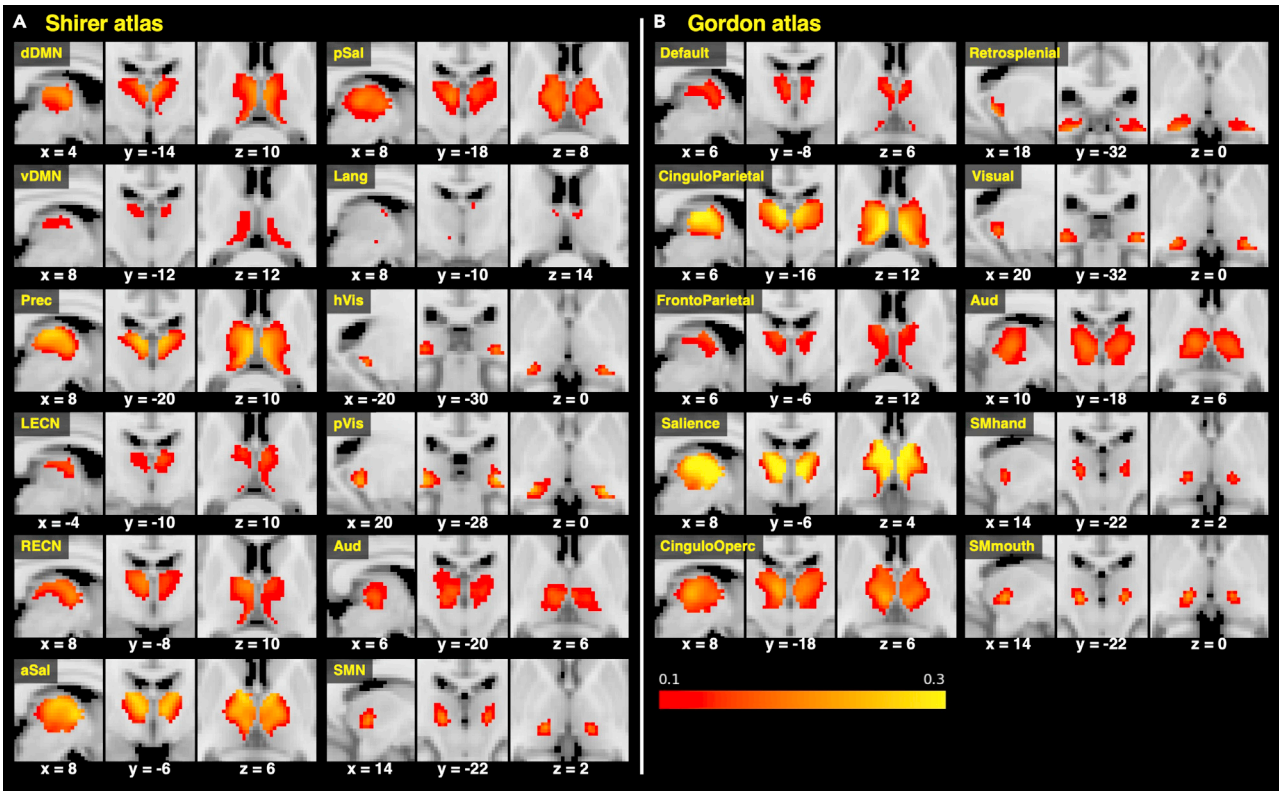

Figure 2. Thalamic regions with strong connections to different resting state networks

Regions shown in red-yellow indicate voxels with mean FCOR value across participants above 0.1 (10%) for resting state networks in (A) Shirer atlas and (B) Gordon atlas.

(A) dDMN, dorsal default mode network; vDMN, ventral default mode network; Prec, precuneus network; LECN, left executive control network; RECN, right executive control network; aSal, anterior salience network; pSal, posterior salience network; Lang, language network; Visu, visuospatial (dorsal attention) network; pVis, primary visual network; hVis, higher visual network; Aud, auditory network; SMN, sensorimotor network.

(B) Default, default mode network; CinguloParietal, cingulo-parietal network; FrontoParietal, fronto-parietal network; Salience, salience network; CinguloOperc, cingulo-opercular network; VentralAttn, ventral attention network; DorsalAttn, dorsal attention network; Retrosplenial, retrosplenial temporal network; Visual, visual network; SMhand, sensorimotor hand network; SMmouth, sensorimotor mouth network; Aud, auditory network. See also Figures S2A and S2B.

RESULTS

Thalamus has extensive functional connections to almost all RSNs

In the analysis, two sets of resting-state network (RSN) templates were employed: one set from Shirer et al. (Shirer et al., 2012) with 13 RSNs and the other from Gordon, et al. (Gordon et al., 2016) with 10 RSNs (Figure S1). For each RSN template, we calculated FCOR values for all voxels in the thalamus and all participants. The mean values across participants for each RSN were then computed. The results for both the Shirer and Gordon atlases are shown in Figure 2 after applying a threshold value of 0.1 or 10% and in Figure S2A for other threshold values (15% and 20%). Results for FCOR values computed at different false discovery rates (see STAR Methods) are shown in Figure S2B. Of all the RSNs examined, the thalamus showed functional connections to all except the visuospatial (dorsal attention) network with the anterior salience network having the most extensive connections with the thalamus and the language network the least. This finding is consistent for both the Shirer and Gordon atlases and for surviving voxels of seed-based functional connectivity analysis results shown in Figure S2A.

Medial and anterior thalamus connects extensively to core neurocognitive networks

For the Shirer atlas (Figure 2A), voxels with significantly higher FCOR values to the core neurocognitive networks (Menon, 2011; Seeley et al., 2007), such as dorsal default mode network (dDMN), ventral default mode network (vDMN), precuneus network (Prec), left executive control network (LECN), right executive control network (RECN), anterior salience network (aSal), and posterior salience network (pSal), were

predominantly located in the thalamus' medial part. In addition, voxels with higher FCOR values to the LECN and RECN were more localized in the anterior portion. Voxels with stronger FCOR to both anterior salience network (aSal) and posterior salience network (pSal) extensively covered the thalamus except the dorsal lateral part. Even at the 20% threshold, a larger number of voxels with significant connections to aSal and Prec still survived. Voxels associated with the language network were located mostly in the anterior medial thalamus but were very limited in extent, even at a threshold value of 10%. These core-neurocognitive-network associated voxels were predominantly related to the anteroventral (AV), lateral posterior (LP), ventral anterior (VA), and ventral lateral (VL) nuclei as well as mediodorsal medial magnocellular (MDm) and mediodorsal lateral parvocellular (MDl) nuclei as defined in the AAL3 atlas (Figure 3A).

Dorsal and lateral thalamus connect to primary processing systems

Voxels with higher FCOR values to sensory processing networks such as the sensorimotor, auditory, and visual networks were mainly located in the dorsal lateral part of the thalamus. The sensorimotor network-associated voxels were localized around pulvinar lateral (PuL), ventral posterolateral (VPL), intralaminar (IL), and pulvinar anterior (PuA); however, the spatial extent was limited. Voxels with higher FCOR values to the auditory network were located across several nuclei such as IL, MDm, MDl, medial geniculate (MGN), PuA, and PuL, while voxels connected to the primary visual and higher visual networks were located in the dorsal lateral thalamus, around lateral geniculate (LGN), MGN, and PuA. No voxels with connections to the visuospatial (dorsal attention) network survived at 10% threshold FCOR value.

Consistent functional spatial topography using another set of RSN templates

The FCOR profile of the thalamus using the Gordon atlas also showed similar distribution. Voxels with significantly higher FCOR values to the core neurocognitive networks (default, fronto-parietal, and cingulo-parietal) of this atlas were similarly located in the medial thalamus, and the distribution of voxels connected to the salience network was also widespread and located in the anterior and medial part of the thalamus (Figure 2B). Stronger FCOR values to the cingulo-parietal and salience networks were also observed with more voxels surviving even at 20% threshold for connections in these networks compared to other networks. Connections to the two sensorimotor networks (hand and mouth related) were located around PuL, PuA, IL, and VPL (Figure 3B). Voxels with higher FCOR values to the visual network were located around LGN, MGN, and PuA, whereas that to the auditory network involved several thalamic nuclei. Like the visuospatial network in the Shirer atlas, no voxels with FCOR values to the dorsal and ventral attention network in the Gordon atlas survived even at 10% threshold.

Connector hubs are primarily located in the medial and anterior thalamus

To identify connector hubs in the thalamus, we binarized the FCOR maps shown in Figure 2 by assigning a value of 1 to voxels with FCOR value exceeding the threshold (FCOR = 0.1) and 0 to the rest. The binarized maps of all RSNs were then combined. The resulting maps are shown in Figure 4 for both the Shirer (Figure 4A) and Gordon (Figure 4B) atlases. Voxels showing a higher RSN count represent connector hubs, which could represent potential sites for functional integration. From the figure, these voxels were mostly located in the anterior and medial thalamus, particularly in AV, LP, MDm, and MDl, which exhibited prominent connections with not just one but multiple RSNs for both Shirer and Gordon atlases. Spider plots of these regions indicating their functional connections to the different RSNs are shown in Figure 5 and in the Figure S3.

Categorization of different connector hubs in the thalamus

We further classified connector hub regions in the thalamus into control-default, cross-control, and control-processing connector hubs shown in Figure 6 (Bagarinao et al., 2020; Gordon et al., 2018). Control-default connector hubs link control and default mode networks, whereas cross-control hubs link different control networks (see STAR Methods). The control-default and cross-control networks existed in the medial and anterior part of the thalamus. Subregions with the highest mean values of both control-default and cross-control were AV, LP, MDl, and MDm. The control-default and cross-control regions were localized in similar regions, and the peak location of the control-default was in the medial part. On the other hand, the control-processing connector hubs, which link control and primary processing networks, were located in the intermediate part of the thalamus. Intriguingly, all types of connector hubs (control default, cross control, and control processing) converged in the intermedial part of the thalamus (Figure 6D). Subregions with the highest number of RSN connections were MDl, MDm, LP, and PuL. The subregions

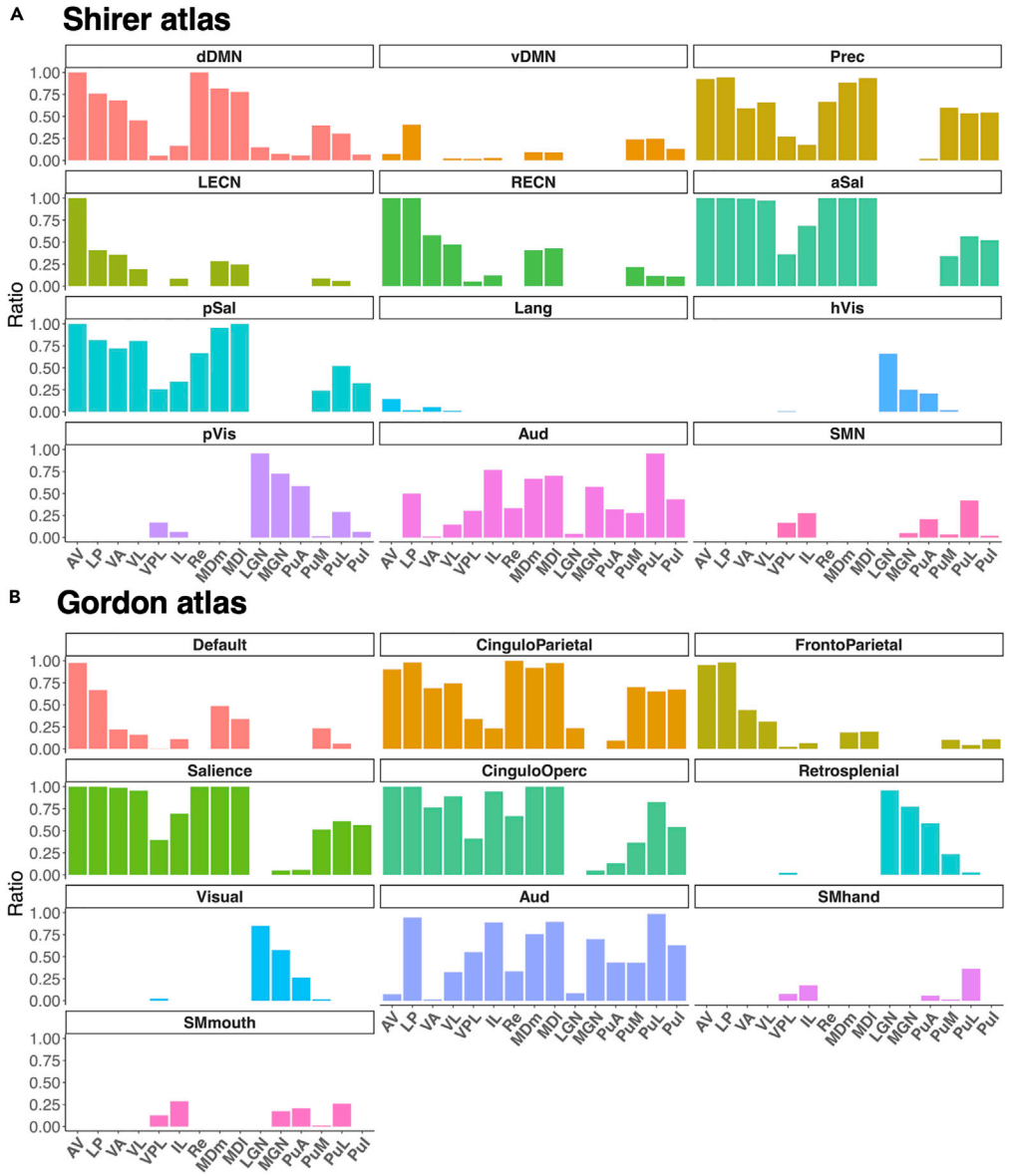

Figure 3. Occupancy ratio of voxels within thalamic subregions that are strongly connected to different resting state networks

Bar graphs indicate the ratio of the number of voxels within each thalamic subregion with mean FCOR values to each RSN greater than 0.1. A value of 1 means that all voxels within the subregion survived the threshold, while a value of 0 means that no voxel survived the threshold. AV, anteroventral; LP, lateral posterior; VA, ventral anterior; VL, ventral lateral; VPL, ventral posterolateral; IL, intralaminar; Re, reuniens; MDm, mediodorsal medial magnocellular; MDl, mediodorsal lateral parvocellular; LGN, lateral geniculate; MGN, medial geniculate; PuA, pulvinar anterior; PuM, pulvinar medial; PuL, pulvinar lateral; Pul, pulvinar inferior.

of LP, MDl, and MDm were associated with both control-default and control-processing hubs, whereas AV and VA were mainly connected to cognitive hubs. The lateral nuclei of LGN, MGN, and PuA were mainly involved in processing networks.

FCOR-based parcellation divides the thalamus into primary processing and cognitive subcomponents

Using FCOR values as voxel features, clustering analysis results are shown in Figure 7. The k value with the highest mean silhouette was 2, followed by 3 in both the Shirer and the Gordon atlases. Using k = 2, the

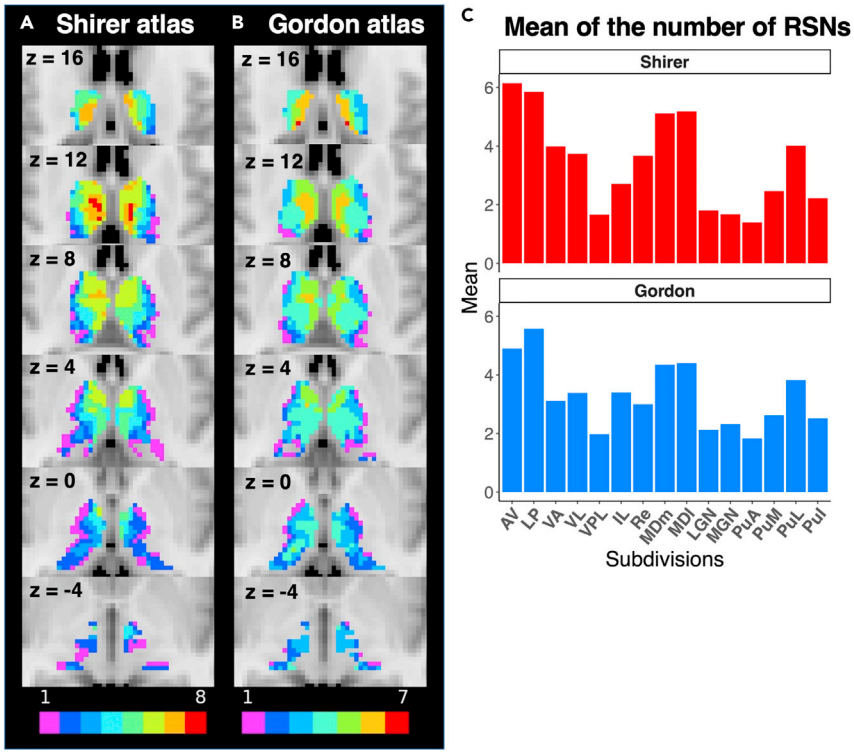

Figure 4. Number of resting-state networks with strong connections to each voxel in the thalamus

(A–C) Color map encodes the number of resting state networks with strong (mean FCOR value >0.1) connections to each thalamic voxel for both the (A) Shirer and (B) Gordon atlases. The mean RSN count within each thalamic subregion is shown in (C).

thalamus was divided into core-neurocognitive thalamus and sensory processing thalamus but with the auditory network-related regions split into an anterior division belonging to the neurocognitive cluster and a posterior division to the sensory processing cluster. Both the Shirer and Gordon atlases provided consistent parcellation. For the 3-cluster parcellation, the thalamus was divided into a core-neurocognitive cluster, sensory processing cluster, and a third cluster involving both cognitive and sensory processing networks. In the Shirer atlas, the third highest mean silhouette was using 4 clusters, followed by 8 clusters (Figures S4 and S5). For 4-cluster parcellation, the two clusters were still predominantly associated with primary processing and neurocognitive networks, while the remaining two were non-specific with components from auditory and salience networks. For the 8-cluster parcellation, the core-neurocognitive associated cluster was further split into two clusters associated with the default mode and executive control networks and the sensory processing cluster into SMN and visual networks. In the Gordon atlas, the k value with the third highest mean silhouette was 5, followed by 8 (Figures S4 and S5). The resulting clusters using the Gordon templates remained relatively consistent with that of the Shirer atlas.

DISCUSSION

Main findings

We examined the functional connections of the thalamus to known RSNs using a FC measure called FCOR. Regions strongly connected to the core-neurocognitive networks that include the default mode, salience, and executive control networks were localized predominantly in the anterior and medial thalamus, such as the anteroventral and mediodorsal nuclei areas. Specifically, regions connected to the salience network covered a more widespread thalamic area, regions connected to the default mode networks were mainly located in the medial thalamus, and to the executive control networks were predominantly in the anterior part. No regions with link to the visuospatial (dorsal attention) network were detected in the thalamus. The sensorimotor network regions were located around the lateral pulvinar nucleus, but the spatial extent was limited. The auditory network regions were localized in the more anterior part than the sensorimotor

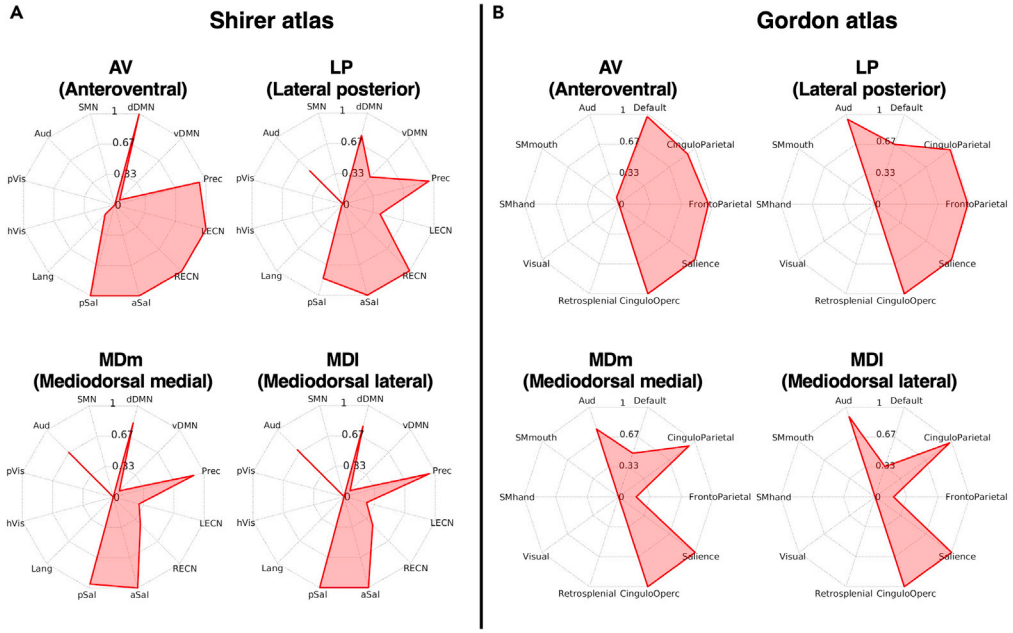

Figure 5. Spider plots of FCOR values for subregions with the 4 highest number of connected resting-state networks

(A–B) Spider plots show the occupancy ratio of the 4 thalamic subregions including the AV, LP, MDm, and MDl with the highest number of overlapped RSNs for the (A) Shirer and (B) Gordon atlases. See also Figure S3.

network and across multiple nuclei. The visual network-related regions were in the dorsal lateral thalamus around the lateral geniculate nucleus. The anteroventral, ventral lateral, and mediodorsal nuclei were prominent as connector hubs with connections to multiple RSNs. Both control-default and cross-control connector hubs were concentrated in these regions, and all types of hubs converged in the intermediate part. Our findings showed that the thalamus is extensively connected to almost all RSNs with the posterior regions mainly associated with primary processing networks while a larger subregion significantly involved in networks associated with cognitive functions.

Identifying connecter hub regions using FCOR analysis

Recent studies have investigated the hub properties of the thalamus (Greene et al., 2020; Hwang et al., 2017). Multiple thalamic subdivisions have been shown to display network properties that could integrate multimodal information across diverse cortical functional networks (Hwang et al., 2017). Some regions were identified as network specific, whereas others were characterized as multi-network integration zones (Greene et al., 2020). In this study, we further categorized the divergent functional integrative hub regions in the thalamus with anatomical subcomponents. In addition, we also classified connector hubs into different categories such as control-processing, control-default, and cross-control and thalamic voxels into clusters, which appeared to be arranged into a topographical motif (Bagarinao et al., 2020; Power et al., 2011) with a cluster associated with the core neurocognitive networks at one end and a cluster associated with primary processing networks at the other end. This provides a more extensive characterization of the functional connectivity profile of the thalamus. To achieve all of these, we used the same FCOR metric. Approaches to identify connector hubs commonly used the network metric called participation coefficient (Guimerà and Nunes Amaral, 2005; Rubinov and Sporns, 2010). Estimating this metric at the voxel-level resolution with nodes reaching hundreds of thousands would be computationally challenging, particularly in terms of memory requirement. There is also the intermediate step of identifying community membership of each node, which requires an additional clustering step. Thus, to minimize the needed computation, an initial brain parcellation would be necessary to reduce nodes to a few hundred, limiting the spatial resolution of identified connector hubs to the size of the parcellation. Identifying connector hubs in the thalamus requires resolution at the voxel level given the overall size of the thalamus as well as its dense and extensive connectivity to the cortex. This problem can be properly addressed by using FCOR, which can be used to identify regions with high between-network connectivity at the voxel level.

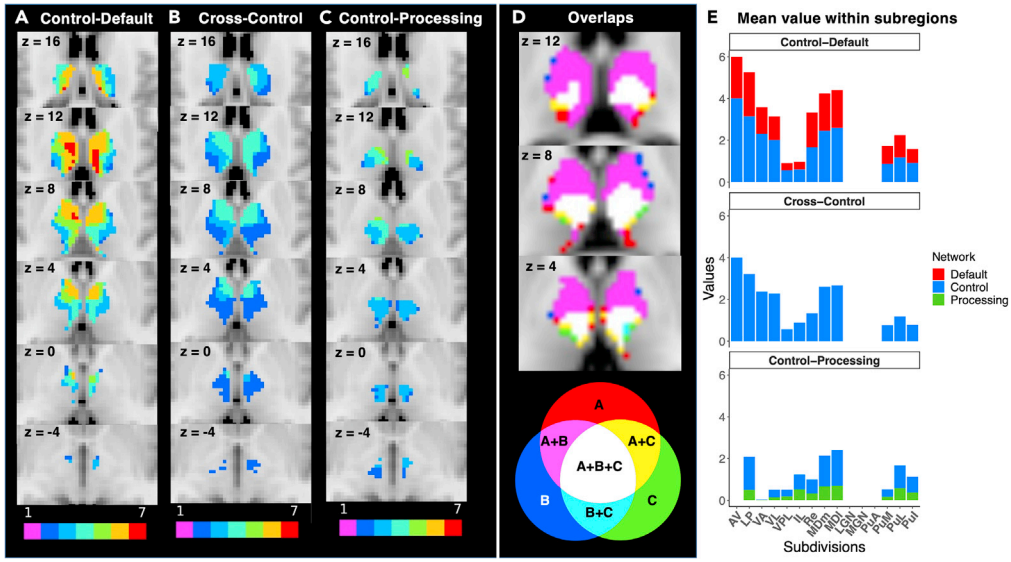

Figure 6. Localization and further categorization of the different connecter hubs in the thalamus

(A–C) Show regions where voxels have strong (mean FCOR value >0.1) connections to at least two resting-state networks belonging to control and default mode networks, control networks, and control and processing networks, respectively, representing (A) control-default, (B) cross-control, and (C) control-processing connector hubs (Gordon et al., 2018; Bagarinao et al., 2020). In control-default and control-processing, voxels with connections to multiple resting-state networks (e.g., dDMN, vDMN, and precuneus networks) belonging to the same general network category (default mode network) are set to 0.

(D) Shows overlap regions among control-default (A), cross-control (B), and control-processing (C). Colors indicate as follows: red – A, blue – B, green – C, magenta – A and B, yellow – A and C, cyan – B and C, white – A, B, and (C)

(E) Shows a voxel-level mean number of overlaps of RSNs related to the control-default, cross-control, and control-processing within each thalamic subregion. Red – default mode, blue – control, green – processing.

Moreover, FCOR can also be independently computed at each voxel so that only FCOR values at specific regions of interest need to be computed as we have demonstrated in this study. Therefore, it enables voxel-level mapping of thalamic hub regions, even though the thalamus is relatively a small structure.

Higher integrative hub regions associated with cognitive processes

We have shown that the anterior subregions of AV and LP and medial parts of MDm and MDl, regions critical for cognitive processing and global amnesia (Mair et al., 2015), were highly connected to multiple RSNs predominantly associated with cognitive processing. The anterior nucleus is a crucial component of the hippocampal system for episodic memory (Child and Benarroch, 2013), and damages of this region manifest memory and language impairment (Nishio et al., 2011). The mediodorsal thalamus is critical for long-term memory and several cognitive functions (Pergola et al., 2018) and closely interacts with the prefrontal cortex in line with multiple cognitive tasks such as working memory, attentional control, and cognitive flexibility (Mitchell, 2015; Mitchell and Chakraborty, 2013; Parnaudeau et al., 2013, 2018; Rikhye et al., 2018; Schmitt et al., 2017). These functions are mostly associated with the default mode and control networks. Thus, our findings showing that cross-control and control-default connector hubs concentrated in the medial and anterior thalamus are consistent with these functional roles, supporting the idea that connector hubs in these regions are critical for cognitive functions.

Thalamic regions linking to core neurocognitive networks

The core neurocognitive networks, including the default mode, salience, and executive control networks, are predominantly connected to the anterior and medial thalamus, such as the anteroventral and mediodorsal nuclei areas, with some networks (salience from both Shirer and Gordon atlases, precuneus, and cingulo-parietal) having high FCOR values (above 20%) in the medial thalamus. The salience network has a crucial role in cognitive control by integrating sensory input to guide attention, attend to motivationally salient stimuli, and recruit appropriate functional networks to modulate behavior (Peters et al., 2016). The salience network also forms a cortico-striato-thalamo-cortical loop, containing the anterior cingulate

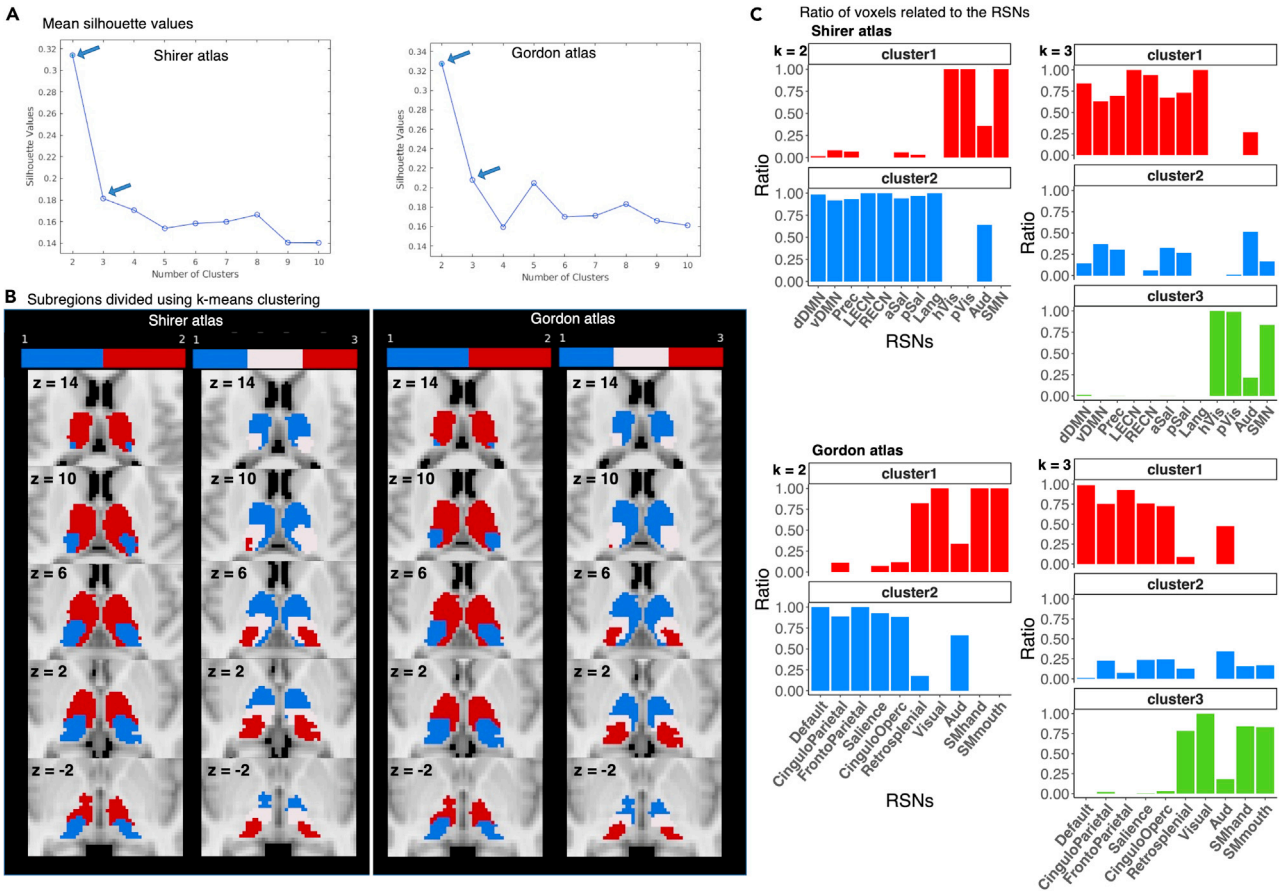

Figure 7. k-means clustering using FCOR values as voxel features in the thalamus

(A) Shows the mean silhouette value as a function of the number of clusters k. Arrows indicate the value of k with the highest and second highest silhouette values.

(B) Shows thalamic parcellation using k-means clustering with 2 and 3 clusters (k = 2 and 3) using FCOR values generated using resting state network templates in the Shirer and Gordon atlases. See also Figure S4.

(C) Shows the ratio of voxels within each parcel with strong (mean FCOR value >0.1) connections to different resting state networks in the Shirer and Gordon atlases. The left column shows the ratio for the 2-cluster parcellation while the right column shows the ratio for the 3-cluster parcellation. See also Figure S5.

and ventral anterior insula as well as the amygdala, hypothalamus, and ventral striatum (Seeley, 2019). A majority of thalamic voxels in the Shirer atlas' anterior salience network and the Gordon atlas' salience network still survived at the 20% threshold suggesting strong connections of these voxels to the salience network. Thalamic connections to the salience network were also more widespread as compared to other networks. As a region that receives input from both subcortical and cortical areas, this result could indicate that the thalamus is an important component of the workings of the salience network.

The precuneus and cingulo-parietal networks, located predominantly in the posterior cingulate cortex and the precuneus, were also functionally connected to the medial thalamus. Functional connections between the precuneus network (posterior default mode network) and medial thalamus have been demonstrated in a previous paper (Yuan et al., 2016), consistent with our study. The precuneus and the thalamus are strongly linked as key components of the default mode network (Cunningham et al., 2017). The mediodorsal thalamic nuclei are anatomically and functionally necessary for the default mode network (Alves et al., 2019). Both regions of the precuneus/posterior cingulate cortex and the mediodorsal thalamus, as well as the pathway between them, are also important for consciousness (Crone et al., 2014; Fernández-Espejo et al., 2012; Hannawi et al., 2015). In our study, the default mode network (the dorsal/ventral default mode and precuneus network) commonly links to the medial thalamus, indicating that this region is essential for the default mode network.

On the other hand, the visuospatial (dorsal attention) network of both the Shirer and Gordon atlases did not show significant connections to the thalamus. This is in contrast to other studies which have shown that the posterior thalamus connects to this network (Yuan et al., 2016) and acts as a site for visual attention integration (Greene et al., 2020). This could be attributed to differences in the methods used. FCOR measures the number of voxels with significant connections to the network rather than the strength (correlation values) of these connections. For the seed-based analysis we performed, the mean time series within the whole network was used to compute the connectivity to the thalamus. Moreover, we also employed a more stringent threshold when estimating the FCOR values. By relaxing the threshold value, we did find regions in the thalamus that were connected to the visuospatial network similar to that in Greene et al. (Greene et al., 2020).

Thalamic regions linking to sensory processing

In the current study, connections to the sensorimotor network were located around PuL, PuA, VPL, and IL; however, regions connected to the SMN were not localized to specific thalamic nuclei in the AAL3 atlas. Existing evidence suggested that the cortico-thalamocortical pathways from the primary to the secondary somatosensory area as well as from the primary somatosensory to the primary motor area involved the posterior medial thalamic nucleus (Mo and Sherman, 2019; Theyel et al., 2010). The ventral intermediate nucleus has also been used as a target for the treatment of medication-resistant tremor symptoms in patients with essential tremor (Elias et al., 2013; Lipsman et al., 2013) and Parkinson disease (Bauer et al., 2014; Schlesinger et al., 2015). This motor integration area in the thalamus has been shown the most successful site for treating essential tremor with deep brain stimulation (Greene et al., 2020). In the present study, regions with connections to the SMN of the Shirer atlas and SM-hand and SM-mouth of the Gordon atlas were consistently located in the same area.

The auditory network, which is related to audition, including tone and pitch discrimination, music, speech, and phonological discrimination (Laird et al., 2011), was connected to multiple thalamic nuclei, including MDm, MDl, MGN, and PuL. These regions contribute to the control-processing hub where multiple RSNs including control and primary processing converged. In the rodent study, the medial geniculate body encodes task, motor, and learning-related information (Gilad et al., 2020). The basal forebrain subcortical projections modulate MGN and play an essential role in auditory processing (Azimi et al., 2020). The medial geniculate body can be divided into three substructures with the ventral part relaying organized information from the inferior colliculus to the primary auditory cortex, while dorsal and medial parts were involved for processing higher complex information (Gilad et al., 2020). Thus, the thalamic regions associated with the auditory network can be considered as multimodal regions.

For visual processing, LGN is the central relay spot for visual information from the retina to the primary visual cortex, consistent with our result showing that this region is functionally connected to the visual processing networks. Moreover, our study showed that PuA was also connected to the visual network. Previous functional and diffusion imaging research revealed distinct thalamocortical connectivity between the dorsal and ventral pulvinar, with the latter shown to have connections to visual cortical areas (Arcaro et al., 2015). Pulvinar is also involved in filtering distracting visual information and highlighting behaviorally relevant targets (Fischer and Whitney, 2012) and is a site to integrate visual areas (Greene et al., 2020). In this study, the control-processing connector hubs were located in the intermediate part of the thalamus, and the posterior lateral thalamus was specific for sensory processing networks. The identified thalamic regions related to the sensory processing-networks were consistent with previous reports (Greene et al., 2020; Hwang et al., 2017).

Thalamic parcellation using FCOR values

Previous studies have performed thalamic parcellation using histological, anatomical, and functional information with the goal of establishing the different thalamic subdivisions based on these criteria. Using resting-state fMRI image, several approaches have been applied to delineate the thalamus, such as cluster analysis (Mezer et al., 2009), independent component analysis (Kim et al., 2013; Kumar et al., 2017; O'Muircheartaigh et al., 2011, 2015), and both seed-based and independent component analyses (Hale et al., 2015). Based on our findings that thalamic substructures have connections to varying functional networks, we used FCOR values to parcellate the thalamus in terms of functional connections. Our result showed a parcellation dividing the thalamus into cognitive-processing and sensory-processing thalamus for 2-cluster analysis. This parcellation was robust irrespective of the RSN atlas used to define the different

RSNs. Using larger k values (parcellation with more than 2 clusters) further delineates specific functional parcellations in the thalamus. Specifically, the parcellation with 3 clusters (k = 3) showed a third region involved in integrative sensory-cognitive processing in addition to the cognitive-processing and sensory-processing regions. This region overlaps with the region where all types of connector hubs converged. The use of FCOR values thus provided the relevant functional information to the different thalamic voxels, whether a given thalamic voxel is primarily involved in primary sensory processing, in multiple-integrative functional processing, or in both.

In conclusion, our results showed that the thalamus is extensively connected to almost all functional networks examined. The anterior and medial thalamus was related to several core neurocognitive-associated networks. In addition, these regions were prominent as connector hubs with connections to multiple large-scale RSNs. On the other hand, the posterior and lateral thalamus was associated mainly with sensory processing networks. Both control-default and cross-control connector hubs were concentrated in the anterior and medial thalamus, and the control-processing hubs localized in the intermediate part. Using FCOR maps, the local functional topography, representing individual connections to different functional brain networks, and the important connector hubs in the thalamus can be clearly identified. This result could serve as a basis for understanding the thalamus' role in typical and atypical brain functions. Overall, our findings suggest that the thalamus, with its extensive functional connections to most of the RSNs, could play an important integrative role that could help facilitate brain functions associated with primary processing as well as higher cognition.

Limitations of the study

We have identified thalamic areas where multiple large-scale cortical networks converged using their functional connectivity profile. These areas, called integrative hubs, may be capable of connecting multimodal brain functions; however, further behavioral or task-based experiments will be needed to ascertain these hubs' integrative functions.

STAR★METHODS

Detailed methods are provided in the online version of this paper and include the following:

- KEY RESOURCES TABLE
- RESOURCE AVAILABILITY
  - Lead contact
  - Material availability
  - Data and code availability
- EXPERIMENTAL MODEL AND SUBJECT DETAILS
  - Participants
- METHODS DETAILS
  - MR settings
  - Image preprocessing
  - Computed functional connectivity overlap ratio (FCOR) in the thalamus
  - Seed-based functional connectivity analysis
  - The number of overlaps RSNs
  - Classification of connector hubs
  - FCOR-based clustering within the thalamus
- QUANTIFICATION AND STATISTICAL ANALYSIS

SUPPLEMENTAL INFORMATION

Supplemental information can be found online at https://doi.org/10.1016/j.isci.2021.103106.

ACKNOWLEDGMENTS

This work was supported by a Grant-in-Aid from the Research Committee of Central Nervous System Degenerative Diseases by the Ministry of Health, Labor, and Welfare; a Grant-in-Aid from the Integrated Research on Neuropsychiatric Disorders project carried out under the Strategic Research for Brain Sciences by the Ministry of Education, Culture, Sports, Science, and Technology of Japan (MEXT); a Grant-in-Aid for Scientific Research from MEXT (grant number: 80569781); and a Grant-in-Aid for Scientific Research on

Innovative Areas (Brain Protein Aging and Dementia Control) (grant number: 26117002) from MEXT. This work was also supported by the Japan Agency of Medical Research and Development (AMED) (grant number: JP21wm0425016).

AUTHOR CONTRIBUTIONS

H.W., S.M., M. Katsuno, T.W., M. Kuzuya, M.H., H.I., S.N., N.O., and G.S. contributed to conception and design of the study. K.K., S.M., D.M., K.H., R.O., M.M., A.O., S.K., M.H., and H.I. were involved in data acquisition, data organization, and data curation. K.K., E.B., H.W., T.T., and H.T. contributed to the methodology, analysis, and interpretation of the data. K.K., E.B., H.W., S.M., and G.S. wrote the draft of the manuscript. All authors reviewed and approved the final version of the manuscript.

DECLARATION OF INTERESTS

The authors declare no competing interests.

Received: March 25, 2021
Revised: August 2, 2021
Accepted: September 2, 2021
Published: October 22, 2021

REFERENCES

Alves, P.N., Foulon, C., Karolis, V., Bzdok, D., Margulies, D.S., Volle, E., and Thiebaut de Schotten, M. (2019). An improved neuroanatomical model of the default-mode network reconciles previous neuroimaging and neuropathological findings. Commun. Biol. *2*, 1–14.

Arcaro, M.J., Pinsk, M.A., and Kastner, S. (2015). The anatomical and functional organization of the human visual pulvinar. J. Neurosci. *35*, 9848–9871.

Azimi, H., Klaassen, A.-L., Thomas, K., Harvey, M.A., and Rainer, G. (2020). Role of the thalamus in basal forebrain regulation of neural activity in the primary auditory cortex. Cereb. Cortex, 1–15.

Bagarinao, E., Watanabe, H., Maesawa, S., Mori, D., Hara, K., Kawabata, K., Yoneyama, N., Ohdake, R., Imai, K., Masuda, M., et al. (2018). An unbiased data-driven age-related structural brain parcellation for the identification of intrinsic brain volume changes over the adult lifespan. Neuroimage *169*, 134–144.

Bagarinao, E., Watanabe, H., Maesawa, S., Mori, D., Hara, K., Kawabata, K., Yoneyama, N., Ohdake, R., Imai, K., Masuda, M., et al. (2019). Reorganization of brain networks and its association with general cognitive performance over the adult lifespan. Sci. Rep. *9*, 11352.

Bagarinao, E., Watanabe, H., Maesawa, S., Mori, D., Hara, K., Kawabata, K., Ohdake, R., Masuda, M., Ogura, A., Kato, T., et al. (2020). Identifying the brain's connector hubs at the voxel level using functional connectivity overlap ratio. Neuroimage *222*, 117241.

Bauer, R., Martin, E., Haegele-Link, S., Kaegi, G., von Specht, M., and Werner, B. (2014). Noninvasive functional neurosurgery using transcranial MR imaging-guided focused ultrasound. Park. Relat. Disord. *20*, S197–S199.

Bell, P.T., and Shine, J.M. (2016). Subcortical contributions to large-scale network communication. Neurosci. Biobehav. Rev. *71*, 313–322.

Child, N.D., and Benarroch, E.E. (2013). Anterior nucleus of the thalamus: functional organization and clinical implications. Neurology *81*, 1869–1876.

Crone, J.S., Soddu, A., Höller, Y., Vanhaudenhuyse, A., Schurz, M., Bergmann, J., Schmid, E., Trinka, E., Laureys, S., and Kronbichler, M. (2014). Altered network properties of the fronto-parietal network and the thalamus in impaired consciousness. Neuroimage Clin. *4*, 240–248.

Cunningham, S.I., Tomasi, D., and Volkow, N.D. (2017). Structural and functional connectivity of the precuneus and thalamus to the default mode network. Hum. Brain Mapp. *38*, 938–956.

Elias, W.J., Huss, D., Voss, T., Loomba, J., Khaled, M., Zadicario, E., Frysinger, R.C., Sperling, S.A., Wylie, S., Monteith, S.J., et al. (2013). A pilot study of focused ultrasound thalamotomy for essential tremor. N. Engl. J. Med. *369*, 640–648.

Fernández-Espejo, D., Soddu, A., Cruse, D., Palacios, E.M., Junque, C., Vanhaudenhuyse, A., Rivas, E., Newcombe, V., Menon, D.K., Pickard, J.D., et al. (2012). A role for the default mode network in the bases of disorders of consciousness. Ann. Neurol. *72*, 335–343.

Fischer, J., and Whitney, D. (2012). Attention gates visual coding in the human pulvinar. Nat. Commun. *3*, 1051.

Gilad, A., Maor, I., and Mizrahi, A. (2020). Learning-related population dynamics in the auditory thalamus. Elife *9*, 1–18.

Gordon, E.M., Laumann, T.O., Adeyemo, B., Huckins, J.F., Kelley, W.M., and Petersen, S.E. (2016). Generation and evaluation of a cortical area parcellation from resting-state correlations. Cereb. Cortex *26*, 288–303.

Gordon, E.M., Lynch, C.J., Gratton, C., Laumann, T.O., Gilmore, A.W., Greene, D.J., Ortega, M., Nguyen, A.L., Schlaggar, B.L., Petersen, S.E., et al. (2018). Three distinct sets of connector hubs integrate human brain function. Cell Rep. *24*, 1687–1695.e4.

Greene, D.J., Marek, S., Gordon, E.M., Siegel, J.S., Gratton, C., Laumann, T.O., Gilmore, A.W., Berg, J.J., Nguyen, A.L., Dierker, D., et al. (2020). Integrative and network-specific connectivity of the basal ganglia and thalamus defined in individuals. Neuron *105*, 742–758.e6.

Guimerà, R., and Nunes Amaral, L.A. (2005). Functional cartography of complex metabolic networks. Nature *433*, 895–900.

Halassa, M.M., and Kastner, S. (2017). Thalamic functions in distributed cognitive control. Nat. Neurosci. *20*, 1669–1679.

Hale, J.R., Mayhew, S.D., Mullinger, K.J., Wilson, R.S., Arvanitis, T.N., Francis, S.T., and Bagshaw, A.P. (2015). Comparison of functional thalamic segmentation from seed-based analysis and ICA. Neuroimage *114*, 448–465.

Hannawi, Y., Lindquist, M.A., Caffo, B.S., Sair, H.I., and Stevens, R.D. (2015). Resting brain activity in disorders of consciousness: a systematic review and meta-analysis. Neurology *84*, 1272–1280.

Hwang, K., Bertolero, M.A., Liu, W.B., and D'Esposito, M. (2017). The human thalamus is an integrative hub for functional brain networks. J. Neurosci. *37*, 5594–5607.

Iglesias, J.E., Insausti, R., Lerma-Usabiaga, G., Bocchetta, M., Van Leemput, K., Greve, D.N., van der Kouwe, A., Fischl, B., Caballero-Gaudes, C., and Paz-Alonso, P.M. (2018). A probabilistic atlas of the human thalamic nuclei combining ex vivo MRI and histology. Neuroimage *183*, 314–326.

Kim, D.J., Park, B., and Park, H.J. (2013). Functional connectivity-based identification of subdivisions of the basal ganglia and thalamus using multilevel independent component analysis of resting state fMRI. Hum. Brain Mapp. *34*, 1371–1385.

Kumar, V.J., van Oort, E., Scheffler, K., Beckmann, C.F., and Grodd, W. (2017). Functional anatomy of the human thalamus at rest. Neuroimage *147*, 678–691.

Laird, A.R., Fox, P.M., Eickhoff, S.B., Turner, J.A., Ray, K.L., McKay, D.R., Glahn, D.C., Beckmann, C.F., Smith, S.M., and Fox, P.T. (2011). Behavioral interpretations of intrinsic connectivity networks. J. Cogn. Neurosci. *23*, 4022–4037.

Lipsman, N., Schwartz, M.L., Huang, Y., Lee, L., Sankar, T., Chapman, M., Hynynen, K., and Lozano, A.M. (2013). MR-guided focused ultrasound thalamotomy for essential tremor: a proof-of-concept study. Lancet Neurol. *12*, 462–468.

Mair, R.G., Miller, R.L.A., Wormwood, B.A., Francoeur, M.J., Onos, K.D., and Gibson, B.M. (2015). The neurobiology of thalamic amnesia: contributions of medial thalamus and prefrontal cortex to delayed conditional discrimination. Neurosci. Biobehav. Rev. *54*, 161–174.

Menon, V. (2011). Large-scale brain networks and psychopathology: a unifying triple network model. Trends Cogn. Sci. *15*, 483–506.

Mezer, A., Yovel, Y., Pasternak, O., Gorfine, T., and Assaf, Y. (2009). Cluster analysis of resting-state fMRI time series. Neuroimage *45*, 1117–1125.

Mitchell, A.S. (2015). The mediodorsal thalamus as a higher order thalamic relay nucleus important for learning and decision-making. Neurosci. Biobehav. Rev. *54*, 76–88.

Mitchell, A.S., and Chakraborty, S. (2013). What does the mediodorsal thalamus do? Front. Syst. Neurosci. *7*, 1–19.

Mo, C., and Sherman, S.M. (2019). A sensorimotor pathway via higher-order thalamus. J. Neurosci. *39*, 692–704.

Mugler, J.P., and Brookeman, J.R. (1990). Three-dimensional magnetization-prepared rapid gradient-echo imaging (3D MP RAGE). Magn. Reson. Med. *15*, 152–157.

Nishio, Y., Hashimoto, M., Ishii, K., and Mori, E. (2011). Neuroanatomy of a neurobehavioral disturbance in the left anterior thalamic infarction. J. Neurol. Neurosurg. Psychiatry *82*, 1195–1200.

O'Muircheartaigh, J., Vollmar, C., Traynor, C., Barker, G.J., Kumari, V., Symms, M.R., Thompson, P., Duncan, J.S., Koepp, M.J., and Richardson, M.P. (2011). Clustering probabilistic tractograms using independent component analysis applied to the thalamus. Neuroimage *54*, 2020–2032.

O'Muircheartaigh, J., Keller, S.S., Barker, G.J., and Richardson, M.P. (2015). White matter connectivity of the thalamus delineates the functional architecture of competing thalamocortical systems. Cereb. Cortex *25*, 4477–4489.

Parnaudeau, S., O'Neill, P.K., Bolkan, S.S., Ward, R.D., Abbas, A.I., Roth, B.L., Balsam, P.D., Gordon, J.A., and Kellendonk, C. (2013). Inhibition of mediodorsal thalamus disrupts thalamofrontal connectivity and cognition. Neuron *77*, 1151–1162.

Parnaudeau, S., Bolkan, S.S., and Kellendonk, C. (2018). The mediodorsal thalamus: an essential partner of the prefrontal cortex for cognition. Biol. Psychiatry *83*, 648–656.

Pergola, G., Danet, L., Pitel, A.L., Carlesimo, G.A., Segobin, S., Pariente, J., Suchan, B., Mitchell, A.S., and Barbeau, E.J. (2018). The regulatory role of the human mediodorsal thalamus. Trends Cogn. Sci. *22*, 1011–1025.

Peters, S.K., Dunlop, K., and Downar, J. (2016). Cortico-striatal-thalamic loop circuits of the salience network: a central pathway in psychiatric disease and treatment. Front. Syst. Neurosci. *10*, 1–23.

Power, J.D., Cohen, A.L., Nelson, S.M., Wig, G.S., Barnes, K.A., Church, J.A., Vogel, A.C., Laumann, T.O., Miezin, F.M., Schlaggar, B.L., et al. (2011). Functional network organization of the human brain. Neuron *72*, 665–678.

Power, J.D., Barnes, K.A., Snyder, A.Z., Schlaggar, B.L., and Petersen, S.E. (2012). Spurious but systematic correlations in functional connectivity MRI networks arise from subject motion. Neuroimage *59*, 2142–2154.

Rikhye, R.V., Wimmer, R.D., and Halassa, M.M. (2018). Toward an integrative theory of thalamic function. Annu. Rev. Neurosci. *41*, 163–183.

Rolls, E.T., Huang, C.C., Lin, C.P., Feng, J., and Joliot, M. (2019). Automated anatomical labelling atlas 3. Neuroimage *206*, 116189.

Rubinov, M., and Sporns, O. (2010). Complex network measures of brain connectivity: uses and interpretations. Neuroimage *52*, 1059–1069.

Schlesinger, I., Eran, A., Sinai, A., Erikh, I., Nassar, M., Goldsher, D., and Zaaroor, M. (2015). MRI guided focused ultrasound thalamotomy for moderate-to-severe tremor in Parkinson's disease. Parkinsons. Dis. *2015*, 1–4.

Schmitt, L.I., Wimmer, R.D., Nakajima, M., Happ, M., Mofakham, S., and Halassa, M.M. (2017). Thalamic amplification of cortical connectivity sustains attentional control. Nature *545*, 219–223.

Seeley, W.W. (2019). The salience network: a neural system for perceiving and responding to homeostatic demands. J. Neurosci. *39*, 9878–9882.

Seeley, W.W., Menon, V., Schatzberg, A.F., Keller, J., Glover, G.H., Kenna, H., Reiss, A.L., and Greicius, M.D. (2007). Dissociable intrinsic connectivity networks for salience processing and executive control. J. Neurosci. *27*, 2349–2356.

Sherman, S.M. (2016). Thalamus plays a central role in ongoing cortical functioning. Nat. Neurosci. *19*, 533–541.

Shine, J.M. (2020). The thalamus integrates the macrosystems of the brain to facilitate complex, adaptive brain network dynamics. Prog. Neurobiol. *101951*.

Shirer, W.R., Ryali, S., Rykhlevskaia, E., Menon, V., and Greicius, M.D. (2012). Decoding subject-driven cognitive states with whole-brain connectivity patterns. Cereb. Cortex *22*, 158–165.

Theyel, B.B., Llano, D.A., and Sherman, S.M. (2010). The corticothalamocortical circuit drives higher-order cortex in the mouse. Nat. Neurosci. *13*, 84–88.

Wolff, M., Morceau, S., Martin-Cortecero, J., Folkard, R., and Groh, A. (2020). A thalamic bridge from sensory perception to cognition. Neurosci. Biobehav. Rev. *120*, 222–235.

Yuan, R., Di, X., Taylor, P.A., Gohel, S., Tsai, Y.H., and Biswal, B.B. (2016). Functional topography of the thalamocortical system in human. Brain Struct. Funct. *221*, 1971–1984.

STAR★METHODS

KEY RESOURCES TABLE

REAGENT or RESOURCE	SOURCE	IDENTIFIER
Software and algorithms		
MATLAB	Mathworks	RRID:SCR_001622; https://www.mathworks.com/products/matlab/
SPM	The Wellcome Centre for Human Neuroimaging, UCL Queen Square Institute of Neurology, London, UK	RRID:SCR_007037; https://www.fil.ion.ucl.ac.uk/spm/
Other		
Resting state network atlas provided by Shirer and colleagues	Shirer et al., 2012	N/A
Resting state network atlas provided by Gordon and colleagues	Gordon et al. 2016	N/A
Automated anatomical labeling 3 (AAL3) atlas	Rolls et al., 2019	N/A
Study Participants	Bagarinao et al., 2018	N/A

RESOURCE AVAILABILITY

Lead contact

Further information and requests for resources should be directed to and will be fulfilled by the Lead Contact, Hirohisa Watanabe (nabe@med.nagoya-u.ac.jp).

Material availability

No new materials were generated for this study.

Data and code availability

- MRI data reported in this paper will be shared by the lead contact upon request subject to the approval of the Ethics Committee of Nagoya University Graduate School of Medicine.
- This paper does not report original code. MATLAB scripts implementing MATLAB and SPM functions will be shared by the lead contact upon request.
- Any additional information required to reanalyze the data reported in this paper is available from the lead contact upon request.

EXPERIMENTAL MODEL AND SUBJECT DETAILS

Participants

We used resting-state fMRI data from 101 healthy participants (64 females) with age ranging from 20 to 49 years who participated in our ongoing healthy aging cohort study (Bagarinao et al., 2018). All participants were cognitively normal with the Mini-Mental State Examination scores above 26 and the Addenbrookes' Cognitive Examination-Revised (ACE-R) scores above 89, with no anatomical abnormality in the brain as seen using MRI, and with less than 0.2 mm mean frame-wise displacement (FD) (Power et al., 2012) of head motion in resting-state fMRI data. All images were inspected by two Japanese board-certified neurologists (HW, KH) and a neurosurgeon (SM).

The study conformed to the Ethical Guidelines for Medical and Health Research Involving Human Subjects endorsed by the Japanese government and was approved by the Ethics Review Committee of Nagoya University Graduate School of Medicine. Written informed consent was obtained from all the participants.

METHODS DETAILS

MR settings

All participants underwent MRI scanning at the Brain and Mind Research Center, Nagoya University using a Siemens Magnetom Verio (Siemens, Erlangen, Germany) 3.0 T MRI scanner with a 32-channel head coil. High-resolution T1-weighted images (T1-WI) and resting-state fMRI data were acquired from all participants (Bagarinao et al., 2018, 2019, 2020). T1-WI were obtained using a 3D Magnetization Prepared Rapid Acquisition Gradient Echo (MPRAGE) sequence (Mugler and Brookeman, 1990) with the following parameters: repetition time (TR) = 2.5 s, echo time (TE) = 2.48 ms, 192 sagittal slices with a distance factor of 50% and 1-mm thickness, a field of view (FOV) = 256 mm, 256 × 256 matrix size, and an in-plane voxel resolution of 1 × 1 mm^2. Resting-state fMRI (RS-fMRI) images were obtained with a gradient-echo (GE) echo-planar imaging sequence using the following parameters: TR = 2.5 s, TE = 30 ms, 39 transversal slices with a 0.5-mm inter-slice interval and 3-mm thickness, FOV = 192 mm, 64 × 64 matrix dimension, flip angle of 80° and 198 total volumes. The participants were instructed to stay awake and close their eyes during the 8-min scan.

Image preprocessing

Image preprocessing was performed using Statistical Parametric Mapping 12 (SPM12; Wellcome Trust Center for Neuroimaging, London, UK; http://www.fil.ion.ucl.ac.uk/spm/software/spm12/). T1-WI images were segmented into component images, including gray matter (GM), white matter (WM), cerebrospinal fluid (CSF), and other non-brain tissue components. Bias-corrected T1-WI and the transformation information from subject space to the Montreal Neurological Institute (MNI) template space were obtained. For functional images, the first five volumes were discarded to account for the initial image instability. The remaining volumes were slice-time corrected relative to the middle slice, and realigned relative to the mean functional image computed after initially realigning the images relative to the first image. The mean image, together with the realigned images, were then coregistered to the bias-corrected T1-WI, normalized to MNI space using the transformation information obtained during segmentation, resampled to an isotropic voxel resolution of 2 × 2 × 2 mm^3, and spatially smoothed using a 6-mm full-width-at-half-maximum 3-dimensional Gaussian filter. Additionally, we regressed out 24 motion-related regressors to correct for head motion given by [Rt, R_t^2, R_{t-1}, R_{t-1}^2], where Rt = [x_t, y_t, z_t, α_t, β_t, γ_t] represents the estimated motion parameters (x, y, and z for translations and α, β, and γ for rotations about x, y, and z, respectively) at time t. We also removed signals within the CSF and WM, the global signal and their derivatives. Finally, a bandpass filter within 0.01–0.1 Hz was applied using in-house MATLAB scripts.

Computed functional connectivity overlap ratio (FCOR) in the thalamus

Using the preprocessed functional images, we calculated the FCOR values relative to a given RSN for all the voxels within the thalamus. The approach was first reported in our previous paper (Bagarinao et al., 2020). For a given voxel within the thalamus, we extracted its time series and computed Pearson's correlation coefficient with the time series of all voxels within the brain. The reference voxel's functional connectivity (FC) map was then generated by applying a threshold to the resulting correlation values using a false discovery rate (FDR) of $q < 0.01$ and including only voxels with significant positive correlation. For a given RSN, we then computed the overlap ratio between the generated FC map and the RSN template using the following equation:

$$FCOR_i^{RSN} = \frac{N_{overlap}}{N_{RSN}}$$

In this equation, the left-hand side represents the *i*th voxel's FCOR value relative to a given RSN, $N_{overlap}$ represents the number of voxels in the *i*th voxel's FC map that overlapped with the RSN template, and N_{RSN} is the number of voxels comprising the RSN template. By repeating the same process for all voxels within the thalamus, an FCOR map associated with a given RSN could be generated. In our previous paper, we investigated several different FDR threshold values and ensured that the peak locations of the map remained consistent (Bagarinao et al., 2020). Here, we additionally generated thalamic FCOR maps using FDR $q < 0.05$ and 0.001 to evaluate the generated map's consistency across different FDR threshold values (Figure S2B).

In this study, we used two sets of RSN templates for the reference RSNs. The first set consisted of 14 RSNs identified using independent component analysis (Shirer et al., 2012). The Shirer RSN templates include the

dorsal default mode network (dDMN), ventral default mode network (vDMN), precuneus network (Prec), left executive control network (LECN), right executive control network (RECN), anterior salience network (aSal), posterior salience network (pSal), language network (Lang), visuospatial (dorsal attention) network (Visu), basal ganglia network (BG), primary visual network (pVis), higher visual network (hVis), auditory network (Aud), and sensorimotor network (SMN). In the following analysis, we excluded the basal ganglia network as well as RSN components within the thalamus and the cerebellum to examine only the cortico-thalamic network features. For the other template, we used the surface-based RSNs provided by Gordon and colleagues (Gordon et al., 2016). The Gordon RSN templates consist of 12 canonical RSNs that included the Default Mode (Default), Cingulo-Parietal (CinguloParietal), Fronto-Parietal (FrontoParietal), Salience, Cingulo-Opercular (CinguloOperc), Ventral Attention (VentralAttn), Dorsal Attention (DorsalAttn), Retrosplenial Temporal (Retrosplenial), Visual, Sensorimotor Hand (SMhand), Sensorimotor Mouth (SMmouth), and Auditory (Aud) networks (https://sites.wustl.edu/petersenschlaggarlab/resources/).

We also used the recently distributed automated anatomical labeling 3 (AAL3) atlas by Rolls and colleagues to identify detailed anatomical thalamic subregions (Rolls et al., 2019). One of the updated features in the AAL3 atlas is the inclusion of thalamic substructures adjusted to the MNI standard space. In this atlas, thalamic substructures were created based on Iglesias and colleagues (Iglesias et al., 2018). They developed a probabilistic thalamic atlas using *ex vivo* brain MRI scans and histological data. Fifteen substructures of the thalamus were included in the AAL3 atlas: Anteroventral (AV), Lateral Posterior (LP), Ventral Anterior (VA), Ventral Lateral (VL), Ventral Posterolateral (VPL), Intralaminar (IL), Reuniens (Re), Mediodorsal medial magnocellular (MDm), Mediodorsal lateral parvocellular (MDl), Lateral Geniculate (LGN), Medial Geniculate (MGN), Pulvinar anterior (PuA), Pulvinar medial (PuM), Pulvinar lateral (PuL), and Pulvinar inferior (Pul) nuclei (Figure S6).

Seed-based functional connectivity analysis

To examine the consistency of FCOR and functional connectivity from seed using each RSN template, we performed seed-based analyses. The time series from all voxels within each RSN were extracted from the preprocessed functional images, and the mean time series was computed. The resulting mean time series was then correlated to the time series of all voxels in the brain. The estimated correlation coefficients were converted into z-scores using the Fisher transform.

The number of overlaps RSNs

To identify connector hub regions in the thalamus, we calculated the number of RSNs showing more than 0.1(10%) spatial overlapped with the thresholded mean FCOR map per voxel. Other threshold values (15% and 20%, respectively) were also investigated. The mean number of overlapped RSNs within different thalamic subregions in the AAL3 atlas was also calculated.

Classification of connector hubs

Among the core neurocognitive networks, we categorized the (dorsal/ventral) default mode and precuneus as ''default mode network,'' and the anterior and posterior salience, right and left executive control, and visuospatial (dorsal attention) networks as ''control network'' (Bagarinao et al., 2020; Gordon et al., 2018). Sensory processing networks including the sensorimotor, auditory, (primary/high) visual networks were categorized as ''processing network.'' Using this general classification of RSNs, we then categorized connector hubs in the thalamus into 1) control-default, linking at least two RSNs belonging to control and default mode network categories, 2) control-processing, for hubs connecting control and processing networks, and 3) cross-control, for hubs linking control-related RSNs. For this, we used a threshold mean FCOR value above 0.1 (10%) to define the connection.

FCOR-based clustering within the thalamus

We also performed k-means clustering using FCOR values within the thalamus using all the participants' data. Specifically, a 2-dimensional matrix was constructed with rows representing the voxels within the thalamus (2083 rows) and columns representing the FCOR values for the 13 RSNs (Shirer atlas) from all participants (13 × 101 columns). To identify the optimal number of clusters to extract, we evaluated the quality of the clusters using silhouette analysis. The number of clusters, k, which gave the highest silhouette value, was chosen. We also examined k values corresponding to the second, third, and fourth highest silhouette values. The same process was performed for the analysis using the Gordon atlas.

QUANTIFICATION AND STATISTICAL ANALYSIS

Individual thalamic FCOR maps were generated using a false discovery rate (FDR) of $q < 0.01$ and including only significant positive correlations when computing FCOR values at each thalamic voxel. FCOR maps were then averaged across participants and connections to different resting state networks were evaluated using mean FCOR value greater than 10% (mean FCOR value >0.1) (Figure 2 and other derived results). Other threshold values (15% and 20%) were also investigated (Figure S2A). In addition, we also generated thalamic FCOR maps using different FDR values ($q < 0.05$ and 0.001) to assess the consistency of the generated maps under different threshold conditions (Figure S2B). In the seed based functional connectivity analysis, we set the threshold of statistical significance at $p < 0.05$, corrected for multiple comparisons using a family-wise error rate (Figure S2A).